DOI: 10.1002/cctc.201000388

CO+NO versus CO+O_2 Reaction on Monolayer FeO(111) Films on Pt(111)

Yu Lei,[a] Mikolaj Lewandowski,[a] Ying-Na Sun,[a] Yuichi Fujimori,[a] Yulija Martynova,[a] Irene M. N. Groot,[a] Randall J. Meyer,[a] Livia Giordano,*[b] Gianfranco Pacchioni,[b] Jacek Goniakowski,[c] Claudine Noguera,[c] Shamil Shaikhutdinov,*[a] and Hans-Joachim Freund[a]

Thin oxide films grown on metal single crystals are used in many "surface science" research groups in attempts to understand the surface chemistry of metal oxides. In addition, these films are employed as suitable supports for modeling highly dispersed metal catalysts (for reviews, see Refs. [1]–[4]). However, in the case of ultrathin films that are only a few angstroms in thickness, the metal substrate underneath the film often affects the properties of metal clusters by charge transfer through the film.[5–8] These observations can, in principle, be traced back to the so-called "electronic theory of catalysis"[9–11] developed in the 1950s and 1960s, and are primarily based on a Schottky barrier model, which predicts, in particular, that by varying the thickness of oxide films, the reactivity of heterogeneous catalysts can be controlled.[11] However, these ideas faded away, primarily because of a lack of successful examples of the promotional effects of thin oxide films on catalytic activity and/or selectivity.

Recently, it has been demonstrated that a thin oxide film grown on a metal may exhibit higher catalytic activity than the metal substrate under the same reaction conditions.[12] Indeed, a thin FeO(111) film grown on Pt(111) is active for CO oxidation at 450 K, a temperature far below that at which Pt(111) itself is active. Furthermore, the rate enhancement was observed on Fe_3O_4-supported Pt nanoparticles,[13] which underwent encapsulation by an FeO(111) film as a result of the strong metal–support interaction.[14]

It has been suggested that, in the millibar pressure range (1 mbar = 100 Pa) of O_2, the bilayer Fe–O film on Pt(111) transforms into a trilayer O–Fe–O film that catalyzes CO oxidation according to a Mars–van Krevelen-type mechanism.[12] A density functional theory (DFT) study corroborated this scenario.[15] The DFT results showed that, by overcoming a small energy barrier of about 0.3 eV, O_2 is chemisorbed on the Fe atom, which is pulled out of the pristine FeO film. In the chemisorbed state, electrons are transferred from the oxide/metal interface to oxygen, resulting in a O_2^{2-} species, which then dissociates, thus forming a local O–Fe–O trilayer structure. Further DFT studies[16] revealed that the reaction is site-specific within the large Moiré unit cell formed due to an approximately 10% mismatch between the FeO(111) and Pt(111) lattices. This mismatch explains scanning tunneling microscopy (STM) results that showed the formation of close-packed O–Fe–O islands rather than a continuous FeO_2 film.[15]

Theoretical modeling showed that CO reacts with the topmost O layer of the O-rich films according to the Eley–Rideal mechanism to form CO_2, which leaves behind an oxygen vacancy upon desorption (this mechanism differs from that predicted for thin MgO(100) films grown on Ag(100)[17]). The activation barrier for CO_2 formation (ca. 0.2 eV) is considerably lower than the computed barrier for the CO oxidation reaction on Pt(111), on the order of 1 eV.[17] Indeed, this finding explains the higher reactivity of the FeO film as compared to Pt at the relatively low temperatures studied here (ca. 450 K). To end the catalytic cycle, the oxygen vacancies must be replenished through reaction with O_2 in the gas phase to restore the FeO_2 film. In principle, this reaction may occur in the same manner as described above for the formation of the FeO_{2-x} film. However, this reaction step has not yet been explicitly studied.

In an attempt to rationalize the unusual reactivity of FeO(111)/Pt(111) in CO oxidation, we focus herein on the CO+NO reaction and compare it with the CO+O_2 reaction, which was studied previously. The comparison revealed interesting behavior that may aid our understanding of the reactivity of ultrathin oxide films.

We first examined the interaction of pure NO with the FeO films. Figure 1 shows the 30 amu (i.e., NO) temperature-programmed desorption (TPD) signal for saturated NO exposure at 100 K. No other products, such as N_2, N_2O, or NO_2, were detected. The NO-TPD spectrum for the clean Pt(111) substrate is also shown for comparison. The latter reproduces well the spectra reported elsewhere,[18] where the peaks at 200 K, 324 K and 373 K were assigned to NO bonded to the threefold hollow hcp sites, on top, and threefold hollow fcc sites, respectively. The TPD spectra show that the FeO surface is essentially inert towards NO under these conditions. The integral amounts of NO adsorbed on FeO at 100 K, as calibrated against NO/Pt(111), correspond to a small coverage of approximately 0.07 ML. Therefore, we tentatively assigned the TPD features at 150–230 K to NO adsorption on defects, as the experiments

[a] Dr. Y. Lei,[+] M. Lewandowski, Y.-N. Sun, Y. Fujimori, Y. Martynova, Dr. I. M. N. Groot, Prof. R. J. Meyer,[++] Dr. S. Shaikhutdinov, Prof. H.-J. Freund
Abteilung Chemische Physik
Fritz-Haber-Institut der Max-Planck-Gesellschaft
Faradayweg 4–6, Berlin 14195 (Germany)
Fax: (+49) 3084134105
E-mail: shaikhutdinov@fhi-berlin.mpg.de

[b] Dr. L. Giordano, Prof. G. Pacchioni
Dipartimento di Scienza dei Materiali
Università di Milano-Bicocca, via Cozzi, 53-20125 Milano (Italy)
Fax: (+39) 0264485400
E-mail: livia.giordano@mater.unimib.it

[c] Dr. J. Goniakowski, Prof. C. Noguera
CNRS and Université Paris 06
UMR 7588, 4 place Jussieu, 75005 Paris (France)

[+] Present address:
Energy Systems Division, Argonne National Laboratory
Argonne, IL 60439 (USA)

[++] Present address:
Department of Chemical Engineering
University of Illinois at Chicago, Chicago, IL 6060 (USA)

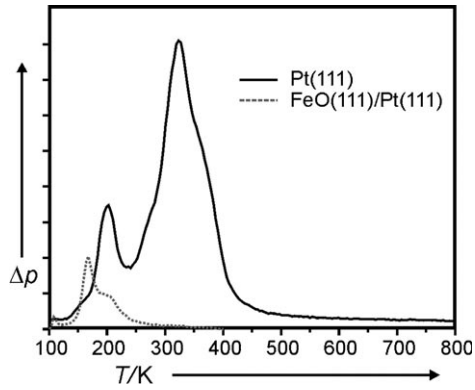

Figure 1. TPD spectra of 7.5 L of NO (30 amu) adsorbed on Pt(111) and FeO(111) at 100 K. The heating rate was 3 K s^{-1}.

with CO on the same samples did not reveal any CO adsorption, which would be indicative of the presence of "holes" in the film.

The films were then exposed to 2 kPa NO in the high-pressure (HP) cell at different temperatures. In contrast to the experiments in ultrahigh vacuum (UHV), at elevated pressures the films became enriched in oxygen in the same manner as previously observed with O_2. Figure 2 shows TPD data from the samples treated in pure NO and pure O_2 at 300 and 450 K. In all cases, two desorption states for O_2 at around 850 K and 1190 K are detected. The high-temperature peak is characteristic for decomposition of FeO films, whereas the peak at 850 K is associated with the topmost O layer in the O–Fe–O films.[15] Only O_2 was detected as a desorbing species in these TPD experiments, indicating that nitrogen is not incorporated into the NO-treated films and implying that, in the course of oxidation at elevated pressures, nitrogen desorbs from the surface, for instance, as N_2. Unfortunately, this process is impossible to monitor in the HP cell with the current setup as the amounts of desorbed molecules during the $FeO \rightarrow FeO_2$ transformation (ca. 10^{15} molecules) are far below the detection limit.

Oxygen enrichment is also monitored by Auger electron spectroscopy (AES) where the O and Fe peak ratio increases upon oxidation by NO and O_2, and matches well the film stoichiometry measured by TPD. Again, no N was detected by AES. Finally, low-energy electron diffraction (LEED) showed that reaction with NO maintains the long-range ordering of the films in the same way as previously found for O_2.

Figure 3 shows STM results obtained on the FeO film exposed to elevated pressures of NO. The images are very similar to those observed for O_2-treated samples. On the large-scale STM image (Figure 3a), wide smooth terraces, separated by monoatomic steps of the Pt(111) substrate, exhibit a superstructure with a periodicity of ca. 2.5 nm like in FeO(111)/Pt(111). The surface is less well ordered than that of the pris-

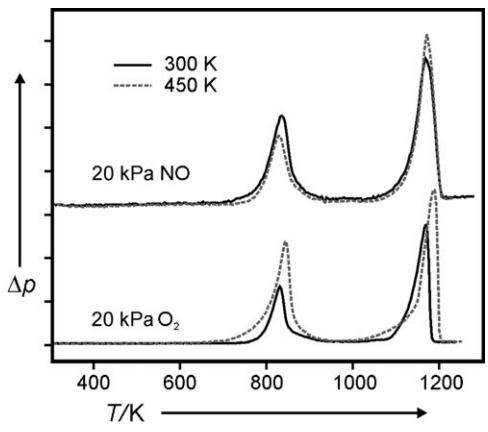

Figure 2. O_2 (32 amu) signal in TPD spectra of FeO films exposed to 2 kPa of NO and O_2 at 300 K and 450 K for 20 min. The heating rate was 3 K s^{-1}.

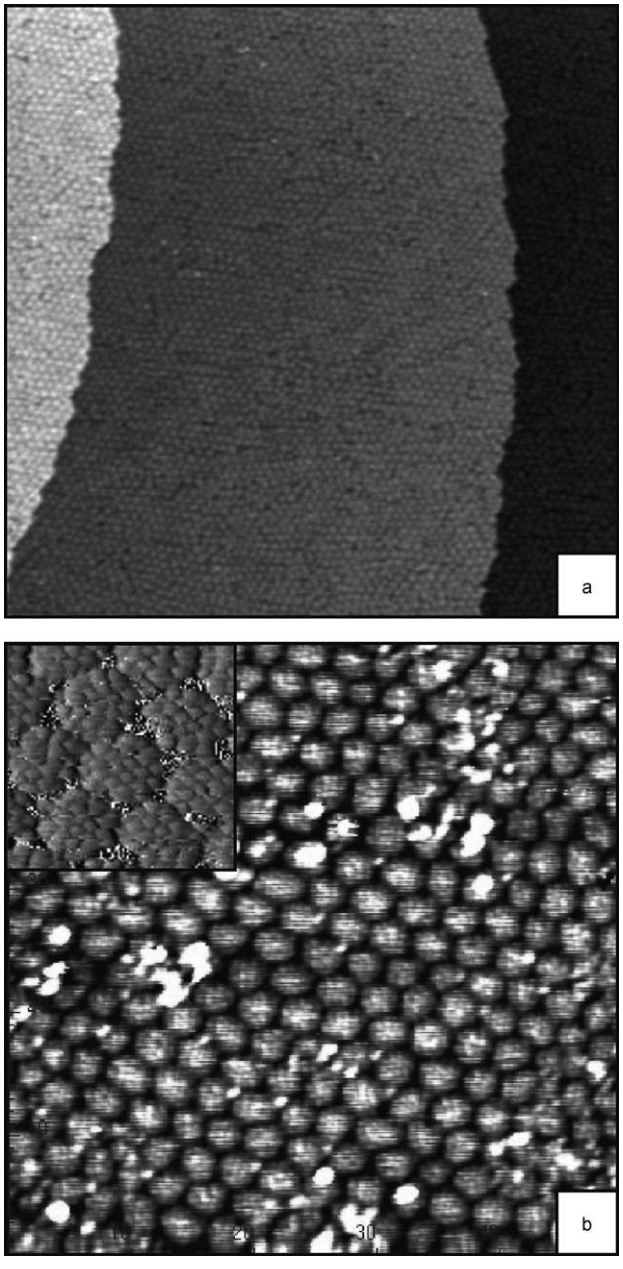

Figure 3. STM images of the FeO(111) film exposed to 200 Pa NO at 450 K for 10 min (a) and 70 Pa NO at 300 K for 1 min (b). The image in the inset, presented by recording the tunneling current channel, zooms in the $(\sqrt{3}\times\sqrt{3})R30^\circ$ superstructure. Image size and tunneling parameters were: a) 200 nm × 200 nm, bias = 1.4 V, current = 0.7 nA; b) 50 nm × 50 nm, 1.0 V, 0.7 nA; inset) 8 nm × 8 nm, 1.0 V, 0.7 nA.

tine FeO films and is represented by close-packed, irregularly shaped islands rather than the film with a wave-like height modulation characteristic of continuous overlayers with a coincident structure to the metal support. As in the case of the O_2-treated films, the islands exhibit a $(\sqrt{3}\times\sqrt{3})R30^\circ$ superstructure (Figure 3b, inset), which has been assigned to relaxation of the Fe ions between two O layers.[16] Therefore, the STM results complemented by LEED, AES, and TPD results, together provide compelling evidence that, at elevated pressures, NO forms an O-rich film, which is virtually identical to that formed by exposure to O_2. This finding is consistent with the thermodynamics of the reaction $FeO+NO\rightarrow FeO_2+{}^1/_2\ N_2$, which is more exothermic than the reaction $FeO+{}^1/_2\,O_2\rightarrow FeO_2$ due to an additional energy gain of approximately 0.9 eV related to the exothermic reaction $NO\rightarrow{}^1/_2\,O_2+{}^1/_2\,N_2$.

Notably, the O/Fe ratio (1.6 ± 0.1) in films treated with 2 kPa NO is almost independent of the reaction temperature, whereas oxidation by 2 kPa O_2 undergoes considerable enhancement (the ratios are 1.5 and 1.9, at 300 and 450 K, respectively). Moreover, STM experiments revealed that the films were transformed across the entire surface at 300 K upon exposure to 70 Pa NO just for 1 min, while the O_2-treated films still exhibited patches of the unreconstructed surface in 0.2 kPa O_2 for 5 h.[15] Therefore, it appears that NO exhibits a lower activation barrier for the $FeO\rightarrow FeO_2$ transformation than O_2.

In the next step, we examined the CO+NO reaction in the millibar pressure range. CO_2 formation in a mixture of 1 kPa CO and 5 kPa NO balanced by He to 0.1 MPa at 450 K is negligible compared to that observed in the 1 kPa CO+5 kPa O_2 mixture. The yield remained almost zero when the FeO film was preconditioned with 2 kPa O_2 at 450 K for 10 min before the reaction in the CO+NO mixture. Meanwhile, the NO pretreated films (2 kPa, 450 K, 10 min) showed the same (high) reactivity in the CO+O_2 reaction. The post-characterization of the spent catalysts showed that after the CO+NO reaction the surface displays a diffuse LEED pattern of Pt(111), whereas a Moiré-like pattern is observed after the CO+O_2 reaction.

To rationalize these results, we address the reaction mechanism proposed for CO oxidation by O_2 on FeO(111)/Pt(111) and assume that the same applies to NO as the oxidative agent:[12,15]

1. O_2 (or NO) transforms the bilayer FeO film into the trilayer FeO_{2-x} film;
2. CO interacts with the outermost O layer, forming CO_2 that desorbs and leaves an oxygen vacancy;
3. O vacancies are replenished by O_2 (or NO) to restore the FeO_{2-x} film.

As the combined AES, LEED, TPD, and STM results showed that the O-rich FeO_{2-x} films produced by O_2 and NO are virtually identical, the remarkable difference in reactivity in CO+O_2 and CO+NO reactions leads to the conclusion that step 3 is the rate-limiting step. Effectively, after the single event in step 2, the CO+NO reaction stops or slows down similarly to the situation in the CO+O_2 reaction under O_2-lean conditions, where the film dewets Pt(111).[12,19] Therefore, disordered and partially reduced films would ultimately be formed, in full agreement with the LEED pattern of the spent catalysts showing diffuse spots of Pt(111). The fact that pretreatment with NO or O_2 does not affect the reactivity (Figure 4) also favors this conclusion as to the identity of the rate-limiting step.

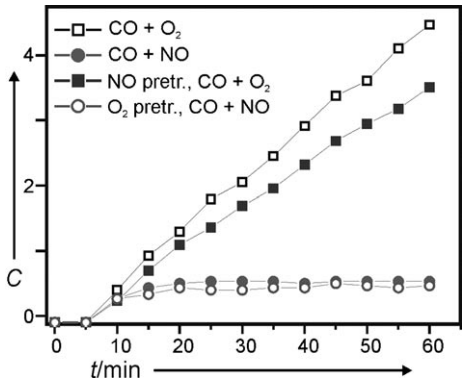

Figure 4. Kinetics of the CO_2 production (C in μmol) over the FeO(111)/Pt(111) film in 1 kPa CO+5 kPa NO and 1 kPa CO+5 kPa O_2 at 450 K. Two samples were pretreated in 2 kPa NO (or O_2) at 450 K for 10 min prior to CO+O_2 (or CO+NO) reaction, as indicated. Time zero corresponds to the start of the sample heating (1 K s^{-1}) from 300 K. All mixtures were balanced to 0.1 MPa by He.

A much lower CO_2 yield in the CO+NO reaction is somewhat surprising since NO is apparently more reactive in step 1 than O_2. To rationalize this effect we performed a DFT analysis of possible reaction pathways.

First, NO adsorption on the perfect FeO_2 surface leads to a NO_2^- complex due to an electron transfer to the metal substrate, which has a sizeable work function. The formed species could, in principle, block CO adsorption at high NO pressures. However, NO-TPD experiments on the FeO_{2-x} films (not shown) revealed that these species become unstable at around 250 K, which is far below the reaction temperature (450 K) and as such hardly contributes to the effect observed.

Previous DFT studies showed that, in a CO+O_2 mixture, the reaction proceeds via the direct interaction of CO with the outermost oxygen of the FeO_2 film,[15] resulting in the formation of an O vacancy after CO_2 desorption (Scheme 1a). An O_2 molecule from the gas phase fills the vacancy and is transformed into a superoxo state (O_2^-). The outermost oxygen atom easily reacts with CO to form CO_2 (Scheme 1b). The formation of CO_2 is highly exothermic (by 4.3 eV) and the reaction proceeds with a negligible activation barrier.

In the case of the CO+NO mixture, the NO molecule binds to a vacancy as strongly as O_2, preferentially in a N-down ge-

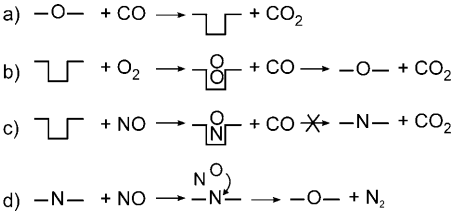

Scheme 1. Reaction pathways on an FeO_2/Pt(111) film (see text for details).

ometry (Scheme 1c), which is about 0.6 eV more stable than O-down adsorption. However, the "dangling" oxygen atom does not easily react with CO, as the reaction must overcome a high (>2 eV) barrier, although the CO_2 formation remains exothermic (by 1.2 eV). Similarly, the "exchange reaction" of a NO molecule with NO adsorbed in the vacancy, resulting in the formation of N_2O and O in the vacancy, is energetically favorable (the gain is about 2.5 eV), but involves an equally high barrier. Therefore, the adsorption of NO at the vacancy kinetically hinders both CO_2 production and the FeO_2 regeneration, thus slowing down the overall reaction as observed experimentally.

Finally, to explain the absence of N in the post-reacted films, we propose the "self-cleaning" mechanism (Scheme 1d). The N atom reacts with ambient NO to form a weakly bound N_2O surface complex. The O atom then moves into the cavity while a N_2 molecule desorbs from the surface. The process is accompanied by a large energy gain (ca. 5 eV) and is essentially non-activated, indicating a very favorable channel for the removal of nitrogen in the film once it has been formed.

In summary, we have shown that NO exposed to FeO(111)/Pt(111) film at elevated pressures readily forms an O-rich, FeO_{2-x} film, which is virtually identical to that formed with O_2. However, negligible CO_2 production in the CO+NO reaction as compared to CO+O_2 is observed, which is rationalized in terms of the replenishment of oxygen vacancies as the rate-limiting step that proceeds much faster with O_2 than NO.

Experimental Section

The experiments were carried out in the same UHV setups used previously and described in detail elsewhere.[12,19] One chamber was equipped with LEED, AES, and TPD apparatus, and housed a small (ca. 30 mL) gold-plated reaction cell connected to a gas chromatograph for reactivity studies at elevated pressures (up to 0.1 MPa). The temperature was measured by a chromel–alumel thermocouple spot-welded to the edge of the double-side polished Pt(111) crystal (10 mm in diameter). CO (99.995%), NO (99.5%), and O_2 (99.999%) were additionally cleaned using a cold trap at about 150 K. The second chamber was additionally equipped with STM apparatus and a preparation cell for high-pressure treatments.

The calculations are based on the DFT+U approach ($U_{Fe}-J_{Fe}=$ 3 eV)[20] using the Perdew-Wang 91 functional[21] as implemented in the VASP code.[22] The FeO_2/Pt(111) film was described with a (2×2) pseudomorphic model, where the interfacial O atoms were placed on top of Pt, which corresponded to the center of the FeO_2 islands observed experimentally.[15,16] In this model, the residual (10%) strain was accommodated in the Pt substrate.[23] As the resulting dilation of the Pt substrate could affect the adsorption properties of the film, the thermodynamics of the processes described in the text were also computed with a nonpseudomorphic model obtained by superposition of $(\sqrt{7}\times\sqrt{7})R19^\circ$ FeO(111) and (3×3) Pt(111) structures.[23] We verified that the energetics computed for these two models are consistent, and the results shown here were obtained only with the pseudomorphic model as reported in Ref. [15]. Reaction profiles were studied by means of the climbing image nudged elastic band method.[24]

Acknowledgements

We acknowledge support from DFG through the Cluster of Excellence UNICAT, coordinated by TU Berlin, and the Fonds der Chemischen Industrie. YL thanks the Max-Planck-Gesellschaft and YF thanks Takata-DAAD for the scholarships. This work was supported by Regione Lombardia and the CILEA Consortium through a LISA Initiative (Laboratory for Interdisciplinary Advanced Simulation) and the Barcelona Supercomputing Center.

Keywords: density functional calculations · heterogeneous catalysis · iron · oxidation · thin films

[1] D. W. Goodman, *Chem. Rev.* **1995**, *95*, 523–536.
[2] C. T. Campbell, *Surf. Sci. Rep.* **1997**, *27*, 1–111.
[3] P. L. J. Gunter, J. W. Niemantsverdriet, F. H. Ribeiro, G. A. Somorjai, *Catal. Rev. Sci. Eng.* **1997**, *39*, 77–168.
[4] H.-J. Freund, *Surf. Sci.* **2002**, *500*, 271–299.
[5] H.-J. Freund, G. Pacchioni, *Chem. Soc. Rev.* **2008**, *37*, 2224–2242.
[6] P. Frondelius, A. Hellman, K. Honkala, H. Hakkinen, H. Grönbeck, *Phys. Rev. B* **2008**, *78*, 085426.
[7] G. Pacchioni, L. Giordano, M. Baistrocchi, *Phys. Rev. Lett.* **2005**, *94*, 226104.
[8] M. Sterrer, T. Risse, U. M. Pozzoni, L. Giordano, M. Heyde, H.-P. Rust, G. Pacchioni, H.-J. Freund, *Phys. Rev. Lett.* **2007**, *98*, 206103.
[9] N. Cabrera, F. Mott, *Rep. Prog. Phys.* **1949**, *12*, 163–184.
[10] F. F. Vol'kenshtein, *Russ. Chem. Rev.* **1966**, *35*, 537–545.
[11] G.-M. Schwab, *Adv. Catal.* **1979**, *27*, 1–22.
[12] Y. N. Sun, Z. H. Qin, M. Lewandowski, E. Carrasco, M. Sterrer, S. Shaikhutdinov, H.-J. Freund, *J. Catal.* **2009**, *266*, 359–368.
[13] M. Lewandowski, Y. N. Sun, Z. H. Qin, S. Shaikhutdinov, H.-J. Freund, *Appl. Catal. A*, DOI: 10.1016/j.apcata.2010.04.030.
[14] a) Z. H. Qin, M. Lewandowski, Y. N. Sun, S. Shaikhutdinov, H.-J. Freund, *J. Phys. Chem. C* **2008**, *112*, 10209–10213; b) Z. H. Qin, M. Lewandowski, Y. N. Sun, S. Shaikhutdinov, H.-J. Freund, *J. Phys. Condens. Matter* **2009**, *21*, 134019.
[15] Y. N. Sun, L. Giordano, J. Goniakowski, M. Lewandowski, Z. H. Qin, C. Noguera, S. Shaikhutdinov, G. Pacchioni, H.-J. Freund, *Angew. Chem.* **2010**, *122*, 4520–4523; *Angew. Chem. Int. Ed.* **2010**, *49*, 4418–4421.
[16] L. Giordano, M. Lewandowski, I. M. N. Groot, Y. N. Sun, J. Goniakowski, C. Noguera, S. Shaikhutdinov, G. Pacchioni, H.-J. Freund, *J. Phys. Chem. C* **2010**, *114*, 21504–21509.
[17] A. Hellman, S. Klacar, H. Grönbeck, *J. Am. Chem. Soc.* **2009**, *131*, 16636–16637.
[18] a) J. L. Gland, B. A. Sexton, *Surf. Sci.* **1980**, *94*, 355–368; b) M. Matsumoto, N. Tatsumi, K. Fukutani, T. Okano, *Surf. Sci.* **2002**, *513*, 485–500; c) C. Xu, B. E. Koel, *Surf. Sci.* **1994**, *310*, 198–208; d) J. F. Zhu, M. Kinne, T. Fuhrmann, B. Trankenschuh, R. Denecke, H.-P. Steinruck, *Surf. Sci.* **2003**, *547*, 410–420.
[19] Y. N. Sun, Z. H. Qin, M. Lewandowski, S. Kaya, S. Shaikhutdinov, H. J. Freund, *Catal. Lett.* **2008**, *126*, 31–35.
[20] S. L. Dudarev, G. A. Botton, S. Y. Savrasov, C. J. Humphreys, A. P. Sutton, *Phys. Rev. B* **1998**, *57*, 1505.
[21] J. P. Perdew, J. A. Chevary, S. H. Vosko, K. A. Jackson, M. R. Pederson, D. J. Singh, C. Fiolhais, *Phys. Rev. B* **1992**, *46*, 6671.
[22] a) G. Kresse, J. Hafner, *Phys. Rev. B* **1993**, *47*, 558; b) G. Kresse, J. Furthmüller, *Phys. Rev. B* **1996**, *54*, 11169.
[23] L. Giordano, G. Pacchioni, J. Goniakowski, N. Nilius, E. D. L. Rienks, H.-J. Freund, *Phys. Rev. B* **2007**, *76*, 075416.
[24] G. Henkelman, B. P. Uberuaga, H. A. Jonsson, *J. Chem. Phys.* **2000**, *113*, 9901–9904.

Received: November 4, 2010
Published online on January 4, 2011

